

INSTRUMENTATION

The Sources of Overestimation in the Quantification by SPECT of Uptakes in a Myocardial Phantom: Concise Communication

Wei Chang, Robert E. Henkin, and Edward Buddemeyer

University of Maryland School of Medicine, Baltimore, Maryland, and Loyola University Medical Center, Maywood, Illinois

A single photon emission computerized tomographic (SPECT) system's overestimation of the tracer concentration in a myocardial perfusion defect was examined by physical phantom studies. An empirical attenuation correction was used to isolate the problem of overestimation from imperfect attenuation correction. The overestimation of defect concentration in our SPECT system was found to come from three sources: software error, finite spatial resolution of the system, and scattered photons generated inside the phantom. The findings confirmed the current belief that the two major problems remaining in quantification with the SPECT technique are attenuation correction and scatter correction.

J Nucl Med 25: 788-791, 1984

The ultimate goal of single photon emission computerized tomography (SPECT) is not only to make high-contrast tomograms, but also to gain quantitative information of radionuclide distribution. In myocardial perfusion imaging, the quantitative spatial and temporal distribution of blood flow in the myocardium is of vital significance to the clinical management of coronary artery disease, as well as in the follow-up of this patient group. The question as to whether SPECT is going to become a useful clinical technique depends largely on whether quantification is possible.

An elegant experimental study performed on dog hearts compared tissue-sample counting with the SPECT approach to quantification under both in vivo and in vitro imaging conditions (1). This study demonstrated that SPECT accurately reflects regional distribution of blood flow in a normal myocardium. However, for all the perfusion defects in the dog hearts, there was always an overestimation of the tracer concentration, the mean error being around 25%. The authors identified the

sources of error to be cardiac motion, partial-volume effect, self-absorption, and attenuation and scatter by the chest wall and structures surrounding the heart. The report estimated that all these sources could, at most, account for a quarter of the total overestimation. The remaining overestimation—about 20% of the normal concentration—could not be explained. They therefore concluded that the quantitative use of SPECT in myocardium perfusion studies was not yet possible, even if perfect attenuation correction could be achieved.

We believe a better way to identify the sources of error in an experimental situation is to use phantom simulations. With the known configuration of a simple phantom under controlled conditions, the complexity of the problem can be reduced to a manageable level and a source of error can be more easily identified.

One of our recent reports on phantom experiments under simulated conditions (2) has shown the linear relationship between concentration and count density obtained by SPECT techniques under simplified conditions. We also observed an overestimation of 31% of the tracer concentration for all the perfusion defects in that experiment. Although the linear relationship seems to imply that quantification is possible provided a calibration line can be estimated, it is essential to find out

Received Aug. 17, 1983; revision accepted Jan. 17, 1984.

For reprints contact: Wei Chang, PhD, Dept. of Diagnostic Radiology, University of Maryland Hospital, 22 South Greene St., Baltimore, MD 21201.

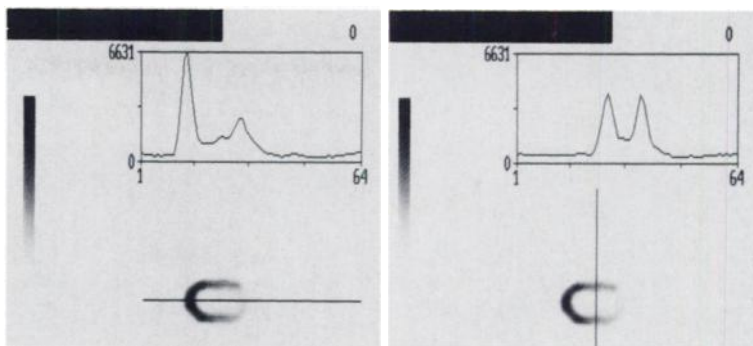


FIG. 1. Central reference tomogram, with its longitudinal (left) and transverse (right) profiles. Note uniform background level outside phantom (which is in air) and non-uniform background inside "ventricle" (which is filled with plexiglas plug).

and account for the causes of the overestimation in the phantom before these results are extended to more general cases. In Ref. 2, a brief speculation on the sources of error was in the discussion, but it provided no direct evidence and it missed a key point.

The purpose of this paper is to provide evidence and analysis that the overestimation in the phantom studies can be explained satisfactorily and totally accounted for by identifying the sources that caused these errors.

MATERIALS AND METHODS

The materials and methods are basically the same as previously described (2). In this similar experiment, the same myocardial phantom containing Tl-201 solution was imaged with the SPECT technique* only in air. However, myocardial perfusion defects were simulated by a pair of balloons, each 15 ml in volume, one containing air and the other plain water. The balloons were placed in opposite myocardial walls of the phantom so that little interference from each other can be assumed in the final analysis of the tomogram. The balloons are compressed between the barrels of the phantom to approximate the shape of a curved disk with 4.5 cm diameter and 1.1 cm thickness. A high-resolution collimator combined with a radius of rotation of 22 cm on our SPECT system leads to a reconstructed spatial resolution of 1.5 cm FWHM. SPECT image acquisition was performed with high count density (12 million counts in 32 views over 180°, in a 64 × 64 acquisition matrix) to reduce random noise. The same imaging was repeated with no balloons in the phantom's wall, and hence with uniform concentration of Tl-201, to provide reference tomograms to facilitate empirical attenuation correction for the perfusion defects under identical conditions. The structure of the phantom ensures that the "ventricular" walls are uniformly thick and contain a known concentration of tracer throughout. The reference tomogram series actually is a quantitative measurement of the attenuation phenomena. By count normalization with respect to the corresponding pixel in the reference tomogram, an ideal attenuation correction can be achieved for each of the perfusion defects.

Profiles were plotted on the central long-axis tomo-

grams of the phantom to examine the quantitative aspect of the mapped images under the various arrangements.

RESULTS

Two profiles of a central longitudinal section of the phantom with no defect are shown in Fig. 1. Part A shows the longitudinal profile along the phantom's axis of symmetry, and part B is a transverse profile cut through the mid-ventricular wall, normal to the long axis. Both profiles reveal that the tomogram has a non-zero, relatively constant background level outside the "heart." This background is about 7% of the primary peak that represents the maximum intensity level at the apex.

Furthermore, both profiles indicate another kind of background, a nonuniform intensity inside the "ventricle," where there is no radioactivity. In Fig. 1A the profile also shows two secondary peaks toward and beyond the "base" of the phantom. The last peak corresponds to the halo at the base, and is as much as 40% of the primary peak.

Figure 2 presents the corresponding tomogram and the transverse profile of the phantom with the two non-radioactive balloons, containing air and water, respectively. The profile was scaled to show the small difference in intensity in the low-intensity range. There are three major intensity peaks in the profile inside the phantom's

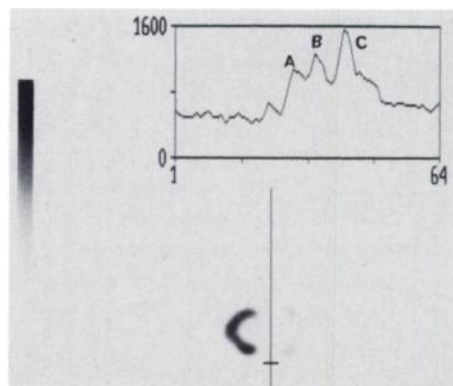


FIG. 2. Transverse profile through defects containing air and water. Profile is scaled to maximum intensity at defect containing water. Three peaks A, B, C, are discussed in text.

cross section, identified as peaks A, B, and C. Peak A corresponds to the location of the phantom wall just outside of the air balloon, while peak C corresponds to the center of the water balloon. Peak B corresponds to the inside of the central plexiglas core and is quite close to the core surface that was in contact with the air balloon.

A quantitative analysis using 3-by-3 regions of interest, placed on this tomogram at the locations of these two air and water balloons defects, has shown the mapped intensity of the defects to be 15% and 20%, respectively, of the maximum intensity at the apex. However, the profile in Fig. 1B shows that attenuation causes the normal wall intensity to drop to 65% of the maximum intensity at the corresponding site of each balloon. Therefore, after attenuation correction, these intensities normalize to 23% and 31% of the normal wall intensity at the mid-ventricular level. On the same basis, the 7% general background outside should normalize to 11%.

DISCUSSION

The experiment we have described was similar to the Seattle group's dog-heart series. We used a myocardial phantom imaged in air with a SPECT system. The phantom image in a simulated chest environment was not included in this paper because we already know that the overestimation would be the same as if the phantom were imaged in air, given proper attenuation correction (2). There was no need for *in vitro* counting because the relative concentration was already expected to be the same. The difference in the radionuclide used is not considered to be significant.

Although we have also observed overestimation of perfusion defects of similar magnitude, in our experiment cardiac motion cannot be its cause. The attenuation correction used in our approach is nearly perfect, so it can be ruled out as a source of error. However, photon spillover from surrounding activities cannot be ruled out because the effective size of our defect (4.5 cm diam) is not much bigger than the FWHM (1.5 cm) of the system's spatial resolution.

From the profile analysis of the tomogram, it is clear that there are several sources that contribute to the overestimate of radionuclide concentration in our SPECT system. The obvious one is the high background bias level that was added after the reconstruction process to mask all the negative pixel values resulting from incomplete cancellation of the background. This is simply a mistake in the software and is to be corrected by the software supplier.

The indicated nonuniform intensity inside the phantom, including the halo beyond its basal portion, is something else. Since the phantom contains no activity in this region, this apparent activity could come only

from scattered radiation and spillover from adjacent activities due to the finite spatial resolution. The halo is caused mainly by photons scattered through the thick plexiglas base plate of the phantom. The other intensities inside the phantom are the combined result of these two sources. Since this observation was found with the myocardial phantom in air, this scatter must have been generated inside the phantom.

The scattered and spillover photons, of course, are not limited to the central portion of the phantom. They are also superimposed on top of the mapped activity in the myocardial walls, and on the simulated defects.

The question now arises: how much does each of these two sources contribute to the overestimation? The answer comes from the experiment with the air and water balloons. When the balloon is full of air, we can assume that no Compton-scattered photon should come from the location of the balloon. Therefore, all the mapped activity in the region of the balloon can be attributed to spillover photons from neighboring activities outside the balloon. Note that the location of the air balloon corresponds to the valley between peaks A and B in the profile of Fig. 2. In the profile, the center of the air balloon shows 23% intensity while the center of the water balloon gives 31% intensity after attenuation correction. We already know that the background bias level accounts for 11% of the overestimation, therefore, the scattered and spillover photons mapped in the tomogram are 8% and 12%, respectively. In other words, the overall overestimation can be broken down to three sources: 11% due to software error, 8% due to Compton-scattered photons, and 12% due to spillover photons in this particular case.

There remains the origin of the central peak B in the profile of Fig. 2. It can be explained as a scatter peak derived from the core of the central Plexiglas cylinder, due to discontinuity in the scattering medium introduced by the air balloon. It subsides as we move further into the core because of photon attenuation.

The magnitude of the spillover-photon contribution observed in this case is in good agreement with the estimation of Whitehead (3). This fact also implies that the spillover contribution to the overestimation is predictable, based on the geometrical dimensions of the defect and the point spread function of the imaging system. The relative contributions of the scattered and spillover photons vary with the radionuclide and the scatter medium's configuration. In the Tl-201 cardiac perfusion tomogram and the defect size that we are usually concerned with, the two components are of the same order of magnitude. For a larger organ with larger photopenic lesions, the scattered component dominates the contribution.

Because of our phantom's symmetry and because the size, shape, and locations of the defects are all similar, the scatter and spillover contributions among all the

defects are quite close in magnitude. This is the reason why we found a linear relationship, as a special case, between the count density and concentration among the defects.

The magnitude of Compton scatter in nuclear medicine imaging has long been overlooked. Its effect on planar imaging and qualitative application of tomography is only to reduce contrast. Rarely does it produce artifacts that are intolerable. For quantitative imaging in a relatively small organ such as the heart, however, it is an important source of error. For primary energies in the 70-keV range, a 60° scattered photon loses only ~4 keV of energy, and the pulse-height analyzer of the imaging system is very poor in rejecting such scattered photons. For 140-keV energies the situation is only slightly better.

Bear in mind that the above explanation for the overestimation caused by scattered and spillover photons only gives us an idea of the origin of the error. To accurately assess these errors in patient studies, further work based on a more sophisticated model will be required. Many other factors, such as lung background and liver, stomach, and blood activity need to be included in the model. These additional considerations can only make the problem more complex and quantification more difficult. However, the point of this paper is to reaffirm the view that SPECT, if it is to be a linear mathematical procedure, should preserve the quantitative aspect of radionuclide concentration. The reason for our overestimation is that the stored data are contaminated with photons of other origins. Since the spillover-photon contribution to the overestimation of focal photopenic imaging can be estimated, the problem remaining for

quantitative SPECT is scatter correction, if a proper attenuation correction can be achieved. This general conclusion applies to other SPECT imaging applications involving large organs. Nevertheless, for an organ such as the heart—which has a relatively simple geometry, especially with symmetry and shell-like radioactivity distribution and an almost isolated location in a not too severely attenuating chest environment—the outlook for proper scatter and attenuation corrections should be optimistic.

FOOTNOTE

* GE 400 AT camera and MDS A² computer system.

ACKNOWLEDGMENTS

We thank Drs. W. L. Rogers for helpful discussion, Tricia Mead for manuscript preparation, and David Crandall for illustration.

REFERENCES

1. CALDWELL JH, WILLIAMS DL, HAMILTON GW, et al: Regional distribution of myocardial blood flow measured by single-photon emission tomography: Comparison with in vitro counting. *J Nucl Med* 23:490–495, 1982
2. CHANG W, HENKIN RE: Photon attenuation in Tl-201 myocardial SPECT and quantitation through an empirical correction. In *Emission Computed Tomography—Current Trends*. Esser PD, ed. New York, Society of Nuclear Medicine, 1983, pp 123–133
3. WHITEHEAD FR: Quantitative analysis of minimum detectable lesion to background uptake ratios for nuclear medicine imaging systems. In *Medical Radionuclide Imaging*. Vol. 1, IAEA, Vienna, 1977, pp 409–434